

# Superparamagnetism and magnetic defects in Fe<sub>2</sub>VAl and Fe<sub>2</sub>VGa

C S Lue<sup>1,3</sup>, Joseph H Ross Jr<sup>1</sup>, K D D Rathnayaka<sup>1</sup>, D G Naugle<sup>1</sup>,  
S Y Wu<sup>2</sup> and W-H Li<sup>2</sup>

<sup>1</sup> Department of Physics, Texas A&M University, College Station, TX 77843-4242, USA

<sup>2</sup> Department of Physics, National Central University, Chung-Li 32054, Taiwan

E-mail: jhross@tamu.edu (J H Ross Jr)

Received 12 October 2000

## Abstract

We have investigated the magnetic properties of Heusler-type Fe<sub>2</sub>VAl and Fe<sub>2</sub>VGa by means of susceptibility, magnetization, and nuclear magnetic resonance (NMR) measurements. As evidenced by the static and dynamic magnetic susceptibilities, both compounds exhibit the characteristic features of a superparamagnetic glass. The freezing temperatures of our samples are 23 K for Fe<sub>2</sub>VAl and 9 K for Fe<sub>2</sub>VGa. A detailed analysis indicates the coexistence of individual magnetic defects with large-moment superparamagnetic clusters. The temperature-dependent magnetization and NMR linewidth are dominated by isolated magnetic defects, identified as Fe antisite defects. The concentration of these defects, determined from NMR linewidths, is  $4.5 \times 10^{-3}$  in Fe<sub>2</sub>VAl, in good agreement with the value deduced from previous field-dependent specific heat measurements.

## 1. Introduction

The Fe<sub>2+x</sub>V<sub>1-x</sub>Al and Fe<sub>2+x</sub>V<sub>1-x</sub>Ga intermetallics have been topics of recent interest due to their unusual magnetic and transport behaviour [1–6]. In both systems, a broad peak in electrical resistivity coincides with an apparent magnetic transition temperature,  $T_c$ , with a negative temperature coefficient of resistivity above  $T_c$  going over to a positive temperature coefficient below the transition [1–6]. However, NMR measurements indicate stoichiometric Fe<sub>2</sub>VAl and Fe<sub>2</sub>VGa to be nonmagnetic semimetals [7, 8], in agreement with theoretical work [9–11]. Therefore, the  $T_c$  for these materials must be due to the presence of magnetic defects, such as those measured via field-dependent specific heat [12].

The behaviour of magnetic defects in Fe<sub>2</sub>VAl and Fe<sub>2</sub>VGa is particularly interesting because of the observation of negative giant magnetoresistance (GMR) for  $T \approx T_c$  [3, 5, 6]. In Fe<sub>2</sub>VGa the GMR effect is near 50%, the highest value reported for magnetically dilute or granular 3d transition metal alloys [5, 6]. It has been suggested that wrong-site Fe atoms

<sup>3</sup> Present address: Department of Physics, National Sun-Yat-Sen University, Kaohsiung, Taiwan.

on V sites (antisite Fe) are magnetic and play a significant role in the magnetism of the two compounds [10, 11]. These antisites have been associated with the  $3.7 \mu_B$  defect identified by specific heat measurements in  $\text{Fe}_2\text{VAl}$  [12], an observation in good agreement with a calculated value of  $3.18 \mu_B$  for this material [11]. The corresponding defect in  $\text{Fe}_2\text{VGa}$  was calculated to have a moment of  $3.2 \mu_B$  [11]. However, Popiel *et al* [13] have found a nonlinear magnetization variation with external fields and an absence of Zeeman splitting in the Mössbauer spectra for  $\text{Fe}_{3-x}\text{V}_x\text{Al}$  with  $0.6 < x < 1.1$ . These observations were associated with a distribution of cluster magnetic moments from 10 to  $10^4 \mu_B$ .

In this work, we report AC susceptibility ( $\chi$ ), DC magnetization ( $M$ ), and nuclear magnetic resonance (NMR) measurements on stoichiometric  $\text{Fe}_2\text{VAl}$  and  $\text{Fe}_2\text{VGa}$ . These results indicate that in addition to magnetic antisite defects, a more dilute population of large-moment clusters is present in these materials. These clusters are found to dominate the low-field susceptibility. Furthermore, a superparamagnetic freezing transition is identified as being associated with these large clusters, explaining the appearance of the low-temperature magnetic transition in these materials.

## 2. Experiments

The samples studied here were prepared by arc melting appropriate amounts of the elemental metals. The  $\text{Fe}_2\text{VAl}$  ingot was annealed in a vacuum-sealed quartz tube at  $1000^\circ\text{C}$  for two days, then annealed at  $400^\circ\text{C}$  for more than 12 h; this was followed by furnace cooling.  $\text{Fe}_2\text{VGa}$  was annealed at  $600^\circ\text{C}$  and then  $400^\circ\text{C}$ . These are the same ingots as were used for previous NMR [7, 8] and specific heat [12] measurements. In a powder x-ray analysis, all observed peaks for both substances could be indexed according to the expected  $\text{L}2_1$  structure. Peak intensities were in good agreement with simulated spectra calculated by standard means. The lattice parameters determined,  $a = 5.76 \text{ \AA}$  for  $\text{Fe}_2\text{VAl}$  and  $a = 5.77 \text{ \AA}$  for  $\text{Fe}_2\text{VGa}$ , are equal to those reported in the literature [1–5, 14, 15]. Powdered samples from these ingots were used for both magnetic and NMR measurements. The grain size for these powders was  $50\text{--}200 \mu\text{m}$ . Wavelength-dispersive spectroscopy (WDS) measurements showed these grains to be uniform in composition, with no signs of phase segregation observed.

### 2.1. NMR linewidths

NMR linewidths can provide a measure of the concentration of magnetic defects in the vicinity of the NMR nucleus [16–18]. Here we show that NMR measurements of  $\text{Fe}_2\text{VAl}$  indicate a concentration of magnetic defects in very good agreement with those found by specific heat measurements in the same sample.

The NMR experiments were performed using a 9 T home-built pulse NMR spectrometer.  $^{27}\text{Al}$  and  $^{51}\text{V}$  NMR spectra were detected at approximately 99 and 101 MHz respectively, in constant field. Powder specimens, mixed with granular quartz to facilitate rf penetration, were placed in thin-walled plastic vials for 4 to 300 K measurements, and in Teflon tubes for high-temperature purposes. Both sample holders showed no observable  $^{27}\text{Al}$  and  $^{51}\text{V}$  NMR signals. The NMR powder patterns were measured by spin-echo integration versus frequency.

For  $\text{Fe}_2\text{VAl}$ , the central portions of the NMR lines exhibited Lorentzian shapes, for both  $^{27}\text{Al}$  and  $^{51}\text{V}$  spectra [7, 19], as expected for broadening by dilute magnetic impurities [17, 18]. We recorded the full width at half-maximum (FWHM) as a measure of the broadening of these lines. For both nuclei, the FWHM increases with decreasing temperature, as illustrated in figure 1(a). These curves can be fitted to a Curie-type term proportional to  $1/T$ , added to

a  $T$ -independent background. Walstedt and Walker have calculated NMR linewidths due to dilute magnetic impurities [18]; for the case where fluctuation of the impurity spins is rapid compared with the NMR splittings, the linewidth is proportional to the average spin moment, giving a Curie-type contribution as observed here. According to this theory, substitutional defects having spin  $S$  and concentration  $f$  will produce a FWHM,  $\Delta\nu$ , which can be expressed as follows:

$$\Delta\nu = \frac{2}{9\sqrt{3}} \frac{\gamma_n \mu_0 f g \mu_B}{V} \langle S_z(T) \rangle \quad (1)$$

where  $\langle S_z(T) \rangle$  is the average moment, and  $V$  the volume per formula unit. We fixed the defects as having  $g = 1.93$  and  $S = 3/2$ , values obtained from specific heat measurements [12]. As described in the introduction, these defects are identified with the Fe antisite. The least-squares fit, shown as a dotted curve in figure 1(a), yields an impurity concentration  $f = 0.0045$ . This value is very close to the value,  $f = 0.0037$ , deduced from the specific heat [12]. The consistency of these results indicates that the same defect is responsible for both effects. The well-defined Schottky anomaly in the specific heat indicates a single defect to be responsible, rather than a collection of defects with a continuum of moments, and the NMR results indicate these Fe<sub>2</sub>VAl antisite defects to be more or less uniformly distributed within the sample.

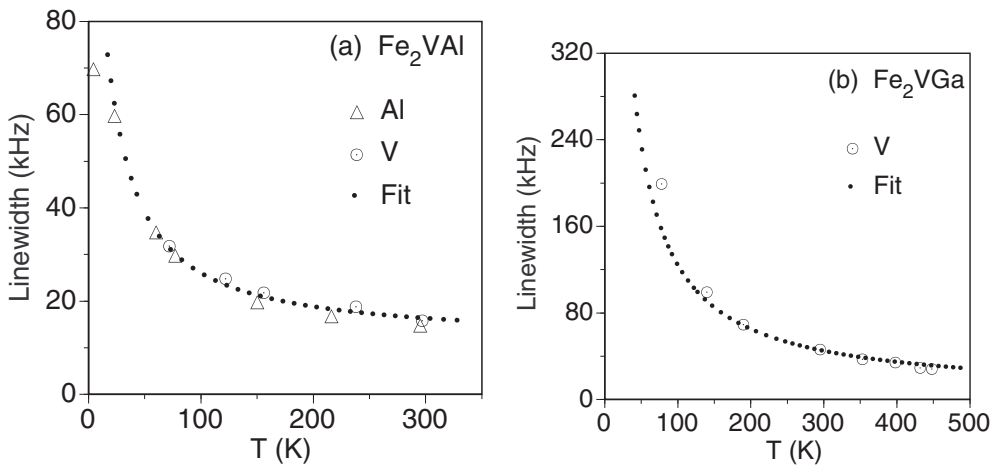


**Figure 1.** The variation of the <sup>27</sup>Al and <sup>51</sup>V FWHM linewidths with temperature for (a) Fe<sub>2</sub>VAl and (b) Fe<sub>2</sub>VGa. Dotted lines: the fit to the broadening described in the text.

<sup>51</sup>V linewidths observed in Fe<sub>2</sub>VGa show a temperature variation similar to those of Fe<sub>2</sub>VAl [8]. However, for the case of Fe<sub>2</sub>VGa, nearly Gaussian lineshapes were observed, as previously reported [8]. The Gaussian lineshape is indicative of a higher concentration of defects [18, 20], for which an analytic solution corresponding to equation (1) is not possible. As an approximate measure [8], we took the FWHM (plotted in figure 1(b)), and fitted the results using the dilute-case solution, equation (1). While specific heat results are not available as an independent measure of the defect distribution in this material, we assumed that the Fe antisites also dominate in Fe<sub>2</sub>VGa. Taking  $g = 1.93$  and  $S = 3/2$  for these defects, the result, drawn as a dotted curve in figure 1(b), gives an impurity concentration  $f \simeq 0.04$  per formula unit.

## 2.2. Magnetic measurements

Susceptibility and magnetization measurements were carried out using a commercial LakeShore magnetometer/susceptometer and a Quantum Design SQUID magnetometer. AC susceptibilities are shown in figure 2 for  $\text{Fe}_2\text{VAI}$  and  $\text{Fe}_2\text{VGa}$ , obtained both in zero field and with the concurrent application of different DC fields as indicated. These data were obtained using an AC excitation field of amplitude 1 Oe and frequency 125 Hz. A prominent maximum in  $\chi$  is observed for  $\text{Fe}_2\text{VAI}$  at 23 K (for zero DC field), while the maximum occurs for  $\text{Fe}_2\text{VGa}$  at 9 K. Both maxima are suppressed by DC fields as small as 10 Oe, as seen in the figure. The measured values of  $\chi$  are significantly larger than expected given the concentrations of antisite defects obtained by means of NMR, quoted above. On the other hand, the susceptibility maxima cannot be associated with bulk ferromagnetic transitions because of the absence of corresponding NMR frequency shifts for either material down to 4 K [7, 8], in measurements previously reported.

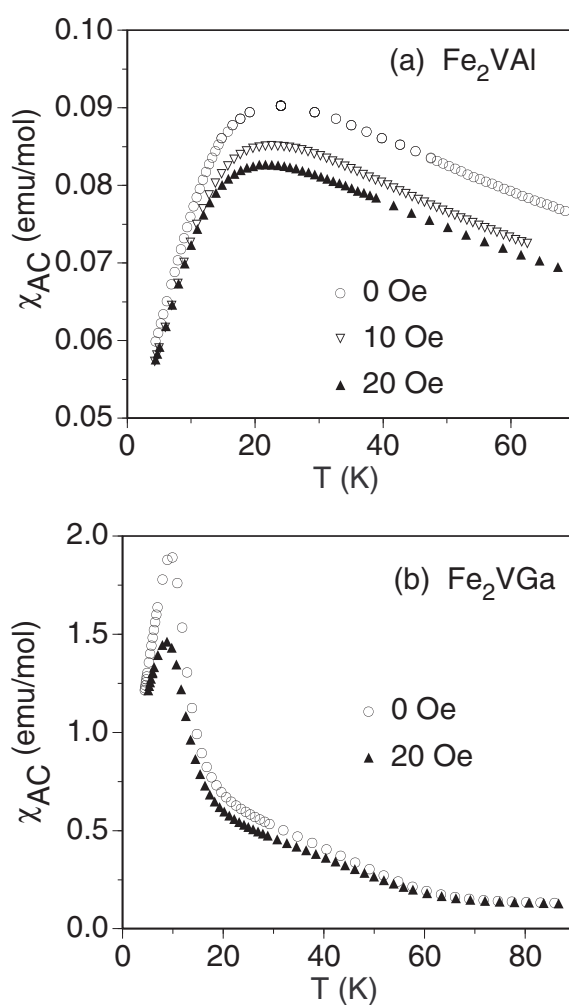


**Figure 2.** Field-dependent AC susceptibilities (real component) for (a)  $\text{Fe}_2\text{VAI}$  and (b)  $\text{Fe}_2\text{VGa}$ . The DC fields indicated were applied during the measurements.

To achieve a further understanding of these results, we measured the frequency dependence of  $\chi$ , with excitation frequencies in the range 1.25 Hz to 1250 Hz. As one can see from figure 3, the amplitude of  $\chi$  has a strong frequency dependence, with the maximum reduced with increasing frequency for each material. This is the characteristic behaviour of spin glasses, for which the frequency dependence is associated with a distribution of energies for spin–spin interactions [21]. However, the large reduction of  $\chi$  with application of a relatively small DC field (figure 2) indicates that the individual moments responsible for the spin-glass-type behaviour are much larger than those of the antisite defects. Therefore, the behaviour observed here is of the superparamagnetic type rather than the spin-glass type.

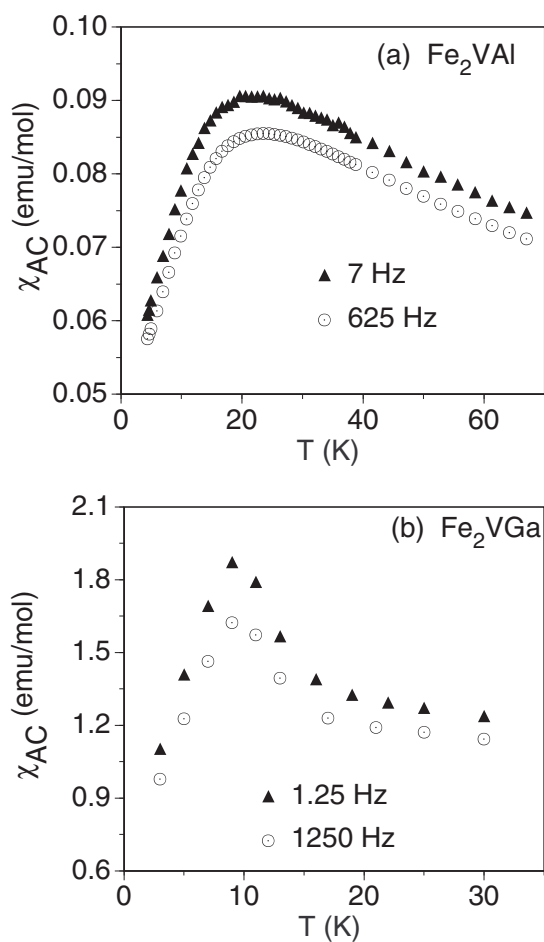


**Figure 3.** AC susceptibility curves for (a) Fe<sub>2</sub>VAl and (b) Fe<sub>2</sub>VGa obtained at the frequencies indicated.

An approximate measure of the size of the superparamagnetic moments present can be obtained from the field dependence of  $\chi$  (figure 2). Assuming superparamagnetic clusters of uniform size, a fit in a narrow temperature range above the maximum in  $\chi$  for Fe<sub>2</sub>VAl yields a moment of 5000  $\mu_B$ , with a concentration of  $10^{-7}$  per formula unit. For Fe<sub>2</sub>VGa this fit yields moments of the same size, 5000  $\mu_B$ , with a concentration of  $10^{-6}$  per formula unit. The Fe<sub>2</sub>VAl result is consistent with Mössbauer results [13] indicating local moments ranging

up to  $10^4 \mu_B$ . On the other hand, a well-defined Schottky anomaly corresponding to antisite defects of  $3.7 \mu_B$  was the only peak apparent in specific heat measurements for  $\text{Fe}_2\text{VAI}$  [12], in agreement with the NMR lineshape fits described above. So, there must be two populations of magnetic defects in  $\text{Fe}_2\text{VAI}$ , rather than a continuous range from small to large moment. These populations include the isolated  $3.7 \mu_B$  Fe antisites, and superparamagnetic moments of approximate average moment  $5000 \mu_B$ . Since the susceptibility maximum is associated with the large moments, we identify it as a superparamagnetic freezing transition [21–24] due to the interactions of large-moment spins.

The presence of large superparamagnetic moments, in addition to the antisite defects, will introduce an additional broadening mechanism for the NMR lineshapes. Superparamagnetic moments of approximate size  $5000 \mu_B$  will be completely polarized in the 9 T NMR field used here, so such moments will give a temperature-independent contribution to the NMR linewidth. With these moments uniformly distributed in the sample, equation (1) can be applied, if  $\langle S_z(T) \rangle$  is replaced by the temperature-independent saturated superparamagnetic moment. This yields an additional contribution of 3 kHz to the NMR linewidth for  $\text{Fe}_2\text{VAI}$ , and 30 kHz for  $\text{Fe}_2\text{VGa}$ , using the superparamagnetic moment concentrations estimated above. These additive contributions to the NMR linewidth are consistent with the measurements, and do not affect the antisite defect estimates given above, since the Curie-law contribution to the linewidths is unaffected.

A measure of the total moment present in these materials is provided by the DC magnetization,  $M$ . Such results are shown in figure 4, for fields up to 7 T, at several temperatures. The dotted curves plotted along with these data were calculated for the lowest and highest measured temperatures for each material (5 K and 160 K for  $\text{Fe}_2\text{VAI}$ , 5 K and 50 K for  $\text{Fe}_2\text{VGa}$ ). In calculating these curves, we made the simplifying assumption of uniform and independent  $5000 \mu_B$  superparamagnetic moments, as well as the antisite defects having  $g = 1.93$  and  $S = 3/2$ . The superparamagnetic moments become saturated below 1 T at all temperatures, giving the rapid rise seen in the data at low fields, while the antisite defects only become appreciably polarized in higher fields, giving the slower rise in  $M$  seen at the lowest temperature. For  $\text{Fe}_2\text{VAI}$ , the defect concentrations obtained from NMR and  $\chi$  give good agreement; the antisites dominate the saturated moment, and for 5 K the curve follows the data well. Departures apparent for the 160 K curve can be attributed to the superparamagnetic moments having a size distribution, rather than the fixed size assumed for the calculation. We have not attempted to fit these data to a specific distribution of superparamagnetic moments.

For  $\text{Fe}_2\text{VGa}$ , an antisite density of 0.02 (rather than 0.04) per formula unit provided better agreement with the  $M$  versus  $H$  data, reflecting the considerable approximation used in applying equation (1) to the NMR results for this material. We also increased the superparamagnetic moment density above the estimate obtained from  $\chi$ , yet the poor fit of the calculated curves to the data indicates a broad distribution of moment sizes, as compared to  $\text{Fe}_2\text{VAI}$ . The data show that the saturation moment of  $\text{Fe}_2\text{VGa}$  is dominated by large moments, as opposed to the case for  $\text{Fe}_2\text{VAI}$ , where the isolated antisite defects dominate. The larger moment in  $\text{Fe}_2\text{VGa}$ , compared to  $\text{Fe}_2\text{VAI}$ , has been noted previously [5].

For the  $\text{Fe}_2\text{VAI}$  sample, we measured the low-field magnetization under field-cooling and zero-field-cooling conditions. This was done in a field of 20 Oe, but with no difference in the magnetization for the two cases, in contrast to the usual behaviour of spin glasses [21]. Superparamagnetic glasses typically also exhibit a divergence between the field-cooled and zero-field-cooled magnetization below the blocking temperature ( $T_B$ ); however, the shapes of these curves depend upon whether magnetocrystalline anisotropy or mutual particle interactions dominate the magnetic behaviour [23, 24]. A peak in the field-cooled curve can occur when dipolar interactions dominate [23], and we attribute the observed behaviour to this situation.

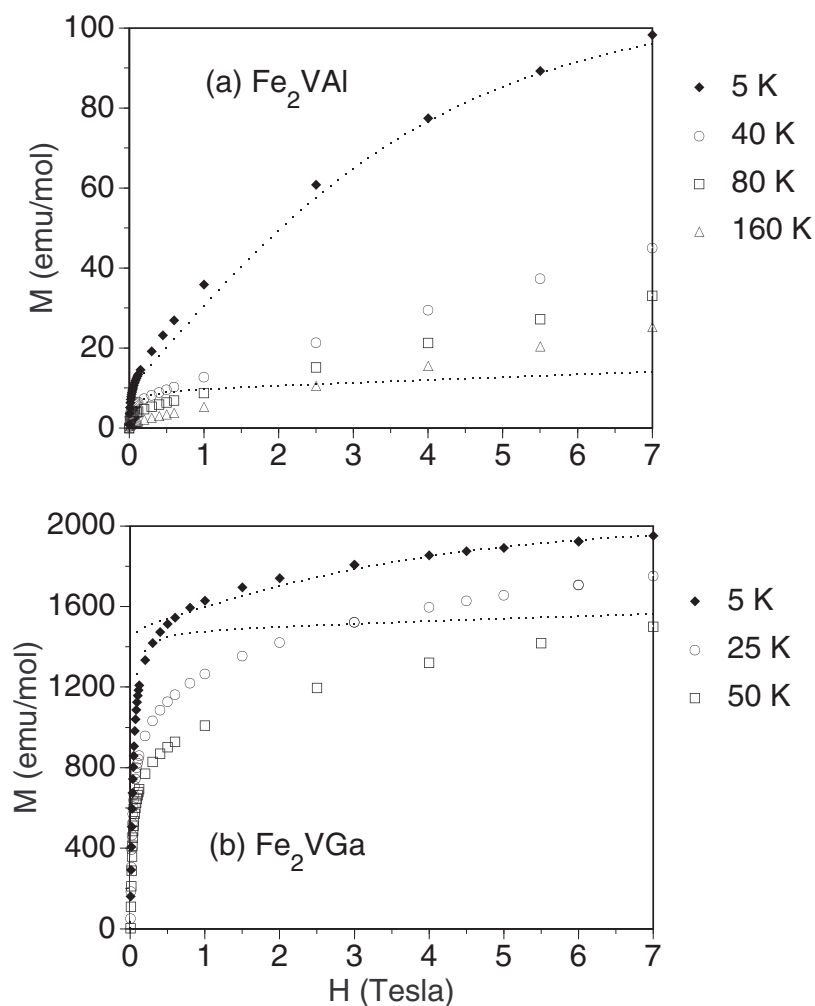


**Figure 4.** DC magnetization versus  $H$  for (a) Fe<sub>2</sub>VAl and (b) Fe<sub>2</sub>VGa measured at the temperatures indicated. Dotted curves: magnetization calculated according to the model described in the text.

### 3. Discussion

Monte Carlo simulations have been reported for dipole-coupled superparamagnetic moments in the Cu–Co system [22]. Scaling the distribution of local fields calculated in that work according to the superparamagnetic moment sizes and concentrations obtained here, we find a typical local dipole field for superparamagnetic moments in Fe<sub>2</sub>VAl equal to 50 Oe. Setting  $T_B$  equal to the temperature at which the thermal energy equals  $\mu H$  in this local field, we obtain  $T_B = 17$  K, which corresponds very well to the observed maximum in  $\chi$  (figure 2). Thus dipolar coupling provides a good explanation of the observed  $T_B$ . The anisotropy may play some role, but surface averaging often serves to minimize the effective anisotropy for nm-sized particles [24]. We noted above that the field-cooled magnetization in Fe<sub>2</sub>VAl, exhibiting a peak at the same temperature as the zero-field-cooled measurement, also points to dipolar interactions as dominant. Since the applied field for that measurement (20 Oe) was smaller than

the estimated local dipole field, it does follow that the field-cooled  $M$  would tend to zero at low temperatures. Note that these are semimetals, so the RKKY interaction will not be effective in coupling the moments. Dipolar coupling is typically most important for superparamagnetic glasses having an insulating matrix [24]. Given the wider distribution of superparamagnetic moments in  $\text{Fe}_2\text{VGa}$ , an estimate of  $T_B$  is more difficult to obtain, but we believe the mechanism for the maximum in  $\chi$  to be essentially the same.

Above 60 K, the field dependence of  $\chi$  for  $\text{Fe}_2\text{VGa}$  disappears, as can be seen in figure 2. We associate this temperature with the internal magnetic ordering temperature ( $T_c$ ) within the superparamagnetic clusters. The corresponding transition is above the range of measurements for  $\text{Fe}_2\text{VAl}$ . To model the origin of superparamagnetic clusters in these materials, we note that both  $\text{Fe}_2\text{VAl}$  and  $\text{Fe}_2\text{VGa}$  have a Fermi level falling inside a narrow pseudogap [7, 8]. With an increase in Fe concentration,  $\text{Fe}_{2+x}\text{V}_{1-x}\text{Al}$  and  $\text{Fe}_{2+x}\text{V}_{1-x}\text{Ga}$  both become ferromagnetic metals. Therefore, fluctuations in the local Fe concentration can lead to regions in which the pseudogap edge is pulled below the Fermi level, creating pockets of ferromagnetic material within the nominally nonmagnetic  $x = 0$  materials. This model is distinct from usual model of superparamagnetic materials, but the pseudogap and nearness to the ferromagnetic composition is a distinctive feature of  $\text{Fe}_2\text{VAl}$  and  $\text{Fe}_2\text{VGa}$ . This model is consistent with the absence of phase segregation observed in these materials, and shows why the magnetic defects can be separated as small and large defects.

Assuming a contribution of  $2\mu_B$  for each Fe in ferromagnetic regions of the sample, the saturation curves (figure 4) can be used to estimate the portion of the sample corresponding to these regions. This estimate yields 1% for  $\text{Fe}_2\text{VGa}$ , and a value about 100 times smaller for  $\text{Fe}_2\text{VAl}$ . Fluctuations in Fe concentration will be dependent upon sample preparation; indeed, Matsushita and Yamada have recently demonstrated that the effect of heat treatment on  $\text{Fe}_2\text{VAl}$  alloys plays a significant role in their magnetic properties [25], in agreement with this assessment. It seems likely that the change from superparamagnetic to ferromagnetic behaviour in  $\text{Fe}_{2+x}\text{V}_{1-x}\text{Al}$  and  $\text{Fe}_{2+x}\text{V}_{1-x}\text{Ga}$  proceeds as a percolation process, as the ferromagnetic regions become larger and eventually encompass the entire sample.

Therefore, the magnetic properties of  $\text{Fe}_2\text{VAl}$  and  $\text{Fe}_2\text{VGa}$  can be interpreted consistently in terms of the following picture: the stoichiometric materials are nonmagnetic, but contain antisite Fe atoms which exhibit local magnetic moments, and also ferromagnetic regions which give the observed superparamagnetic behaviour. The antisite defects produce a  $T$ -dependent contribution to the NMR linewidth, and are responsible for the reported GMR effect [5,6]. The Schottky anomaly in the specific heat of  $\text{Fe}_2\text{VAl}$  has been associated with the same defects [12]. The superparamagnetic regions are associated with the observed magnetic transitions, shown to be magnetic freezing transitions in both  $\text{Fe}_2\text{VX}$  compounds. The observed  $T$ -independent  $\chi$  at high temperatures can be attributed to Van Vleck paramagnetism, consistent with NMR studies [7,8], indicating the Pauli susceptibility to be small.

#### 4. Conclusions

A study of the magnetic properties of  $\text{Fe}_2\text{VAl}$  and  $\text{Fe}_2\text{VGa}$  by means of susceptibility, magnetization, and NMR shows that the magnetic defects in these materials are of two types: large ferromagnetic clusters, and Fe antisite defects. The presence of the antisite defects is indicated by the  $T$ -dependent NMR linewidth, and they are also responsible for the previously reported GMR behaviour. On the other hand, the bulk magnetic behaviour of these materials is dominated by large clusters which exhibit superparamagnetic behaviour, and a low-temperature freezing transition in both materials.

## Acknowledgment

This work was supported in part by the Robert A Welch Foundation (A-0514).

## References

- [1] Nishino Y, Kato M, Asano S, Soda K, Hayasaki M and Mizutani U 1997 *Phys. Rev. Lett.* **79** 1909
- [2] Kato M, Nishino Y, Mizutani U and Asano S 2000 *J. Phys.: Condens. Matter* **12** 1769
- [3] Matsuda H, Endo K, Ooiwa K, Iijima M, Takano Y, Mitamura H, Goto T, Tokiyama M and Aria J 2000 *J. Phys. Soc. Japan* **69** 10
- [4] Kawamiya N, Nishino Y, Matsuo M and Asano S 1991 *Phys. Rev. B* **44** 12 406
- [5] Endo K, Matsuda H, Ooiwa K, Iijima M, Ito K, Goto T and Ono A 1997 *J. Phys. Soc. Japan* **66** 1257
- [6] Endo K, Matsuda H, Ooiwa K, Iijima M, Goto T, Sato K and Umehara I 1998 *J. Magn. Magn. Mater.* **177–181** 1437
- [7] Lue Chin-Shan and Ross J H Jr 1998 *Phys. Rev. B* **58** 9763
- [8] Lue C S and Ross J H Jr 2001 *Phys. Rev. B* **63** 054420
- [9] Weht R and Pickett W E 1998 *Phys. Rev. B* **58** 6855
- [10] Singh D J and Mazin I I 1998 *Phys. Rev. B* **57** 14 352
- [11] Bansil A, Kaprzyk S, Mijnaerends P E and Toboła J 1999 *Phys. Rev. B* **60** 15 132
- [12] Lue C S, Ross J H Jr, Chang C F and Yang H D 1999 *Phys. Rev. B* **60** R13 941
- [13] Popiel E, Tuszynski M, Zarek W and Rendecki T 1989 *J. Less-Common Met.* **146** 127
- [14] Buschow K H J and van Engen P G 1981 *J. Magn. Magn. Mater.* **25** 90
- [15] Webster P J and Ziebeck K R A 1983 *Phys. Lett. A* **98** 51
- [16] Slichter C P 1990 *Principles of Magnetic Resonance* (New York: Springer)
- [17] Kittel C and Abrahams E 1953 *Phys. Rev.* **90** 238
- [18] Walstedt R E and Walker L R 1974 *Phys. Rev. B* **9** 4857
- [19] Lue C S and Ross J H Jr 2000 *Phys. Rev. B* **61** 9863
- [20] Noakes D R 1991 *Phys. Rev. B* **44** 5064
- [21] Binder K and Young A P 1986 *Rev. Mod. Phys.* **58** 801
- [22] Bewley R I and Cywinski R 1998 *Phys. Rev. B* **58** 11 544
- [23] Chantrell R W, Walmsley N S, Gore J and Maylin M 1999 *J. Appl. Phys.* **85** 4340
- [24] Dormann J L, Fiorani D and Tronc E 1997 *Adv. Chem. Phys.* **98** 283
- [25] Matsushita A and Yamada Y 1999 *J. Magn. Magn. Mater.* **167–169** 669